Submicron Crystals of the Parkinson's Disease *Substantia nigra*: Calcium Oxalate, Titanium Dioxide and Iron Oxide

Adam Heller* and Sheryl S. Coffman

McKetta Department of Chemical Engineering, University of Texas, Austin TX 78712 USA

*heller@che.utexas.edu

Abstract

Parkinson's disease (PD) results of the death of dopaminergic neurons of the *substantia nigra*. When activated, the NLRP3 inflammasome of phagocytes releases inflammatory agents, their release resulting in the death of proximal cells. The hallmark protein of PD, aggregated α-synuclein, is phagocytized and activates the NLRP3 inflammasome. Because crystalline particles are known to activate the NLRP3 inflammasome, to enhance α-synuclein expression and aggregation in dopaminergic neurons and because their facets may mis-template adsorbed α-synuclein, we probe here, by transmission electron microscopy (TEM), four human PD *substantia nigra* specimens for their crystalline particles. Samples weighing 5 mg of PD stages 1, 2, 4 and 5 were processed by proteolysis and centrifugation. TEM-grids were dipped in the centrifugate diluted to 1 mL and the dried films were searched for crystalline particles. Two types of crystalline particles, known to activate the NLRP3 inflammasome were found. Endogenous calcium oxalate, a downstream product of ascorbate and dopamine oxidation-produced hydrogen peroxide; and TiO_2, the with pigment of foods and medications. The number-density of the NLRP-inflammasome activating crystalline particles found approached the reported about-equal number-densities of microglia and neuronal cells in the brain.

The observations of COD and protein-coated TiO_2 support two putative feedback loops, both leading to dopaminergic neuron death. In one, polymeric oxidized-dopamine catalyst accelerates H_2O_2-generation, the H_2O_2 indirectly oxidizing ascorbate in an ascorbate-fueled, oxalate-generating, loop the excess oxalate precipitating the subsequently inflammasome-activating COD crystals; In the second, protein-adsorbing facets of TiO_2 mis-template the aggregation of α-synuclein to produce inflammasome-activating mis-folded α-synuclein.

Introduction

Parkinson's disease (PD) results of the degeneration of dopaminergic neurons of the *substantia nigra*. Studies of the past 5 years have shown that a cause of the degeneration is inflammatory attack of dopaminergic neurons of the *substantia nigra* by microglia when their NLRP3 inflammasome is activated by phagocytized misfolded α-synuclein. [1-12] The misfolded β-sheet–rich α-synuclein aggregates in PD's hallmark Lewy bodies. If misfolded α-synuclein templates the misfolding of more synuclein, it constitutes a PD-propagating prion.[13-15] Because phagocytized crystals have been shown to activate the NLRP3 inflammasome [16-25], because they enhance in dopaminergic neurons α-synuclein expression and aggregation, [26] and they adsorb and orient peptides and as well as proteins,[27-29] we probe here by TEM if there are in the human PD *substantia nigra* crystals. We find ghosts of hydrated calcium oxalate (COD) and protein-coated titanium dioxide (TiO_2) crystals. COD is the only non-phosphate containing crystalline insoluble calcium compound in mammalian tissues. It is a long-known cytotoxic component of urinary tract and kidney calculi, [30-32] associated also with retinopathy.[33, 34] Both COD and TiO_2 are phagocytized, [25, 35-39] TiO_2 also by microglia. [40] Both activate the NLRP3 inflammasome. [24, 25, 38, 41-47] Crystalline COD is associated with human lesions [31, 33, 34, 48-50] and has been reported in the human brain, [51] particularly when patients are lethally poisoned by the antifreeze ethylene glycol.[52-54] Ethylene glycol is metabolized to oxalic acid [55, 56] and is precipitated in the brain as calcium oxalate [57]. Ethylene glycol poisoning has induced PD symptoms in a patient.[58]

TiO_2 is the dominant white pigment of foods and medications. It has been detected in brains of animals ingesting or inhaling the submicron-diameter pigment particles.[35, 59-61] In zebrafish larvae submicron TiO_2 particles increased the expressions of PD's hallmark Lewy body formation-associated *pink1*, *parkin*,

α-syn and *uchl1* and caused loss of dopaminergic neurons. [62] Treatment of dopaminergic neurons with TiO_2 increased their α-synuclein expression and caused aggregation of α-synuclein in a dose-dependent manner. [26] TiO_2 adsorbs and orients peptides and proteins. [27-29]

Materials and Methods

Four *substantia nigra* containing specimens of PD stages 1, 2, 4 and 5 were received from the NIH Harvard NeuroBioBank. Of each, 5 mg of each was excised and processed for TEM in plastic-ware free of crystalline matter. The minced samples were digested overnight at ambient temperature with 0.5 mL of an aqueous solution of 5 mg of trypsin (from bovine pancreas, Sigma catalog number 1426) and 5 mg of proteinase K (from *Tritirachium album*, Sigma catalog number P2308). The digested suspensions were centrifuged at 12,000g for 1 hour then the precipitate, with 0.5 mL added water, was dispersed in the resulting 1 mL volume. A 3-mm diameter, 314 square, 200 mesh, copper TEM grid with type-B carbon support (Ted Pella Redding CA, catalog number 1810) was dipped in the resulting 1 mL homogeneous dispersion and dried. The dipping and drying resulted in a residual protein, DNA and other biological matter containing film of a thickness that was about similar to that when a ~10 μL droplet was applied to the 3 mm 314-square grid. To rule out lab-ware-, water- and reagent-associated crystal contamination, samples without tissue were identically processed and were applied to TEM grids. No crystalline particles were observed.

A JEOL 2010F Transmission Electron Microscope (TEM) was used for imaging the particles. Their crystallinity was confirmed by their electron diffraction or by their energy-dispersive X-ray spectroscopic elemental analysis showing > 40 weight % of their metallic element. The TEM search protocol involved location darker, higher atomic-mass, and sharp-edged objects and elemental assay of their selected areas

by energy dispersive X-ray spectroscopy and probing for electron diffraction by their crystalline lattices. The typical TEM time required to locate and characterize one crystalline particle was 2-3 hours. Squares of the 314-square grid were searched until 6 or more crystalline particles were found. In the grids of the PD stages 1 and 2 specimens, search of 3 squares was required; one square of the PD stage 4 grid was searched; and because the first PD stage 5 square searched had numerous particles (Figure 1) only part of it was searched. The apparent increase un the number of crystalline particles per square with the PD stage is likely misleading, because the distribution of crystalline particles on the dipped and dried TEM grid can be non-uniform.

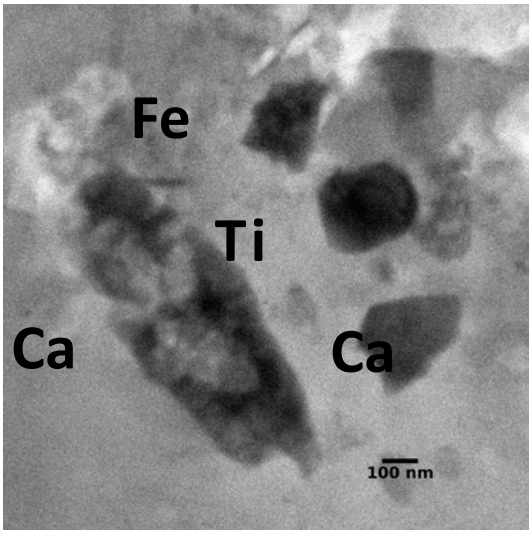

Figure 1. TEM showing multiple crystalline particles in the imaged field of a square of the PD stage 5 grid. The two calcium-rich crystals do not contain phosphorus; the titanium-rich crystal is protein-coated TiO_2; the iron-rich crystal is Fe(O)OH.

Results

Submicron crystalline particles were observed in all four PD *substantia nigra* specimens. The 3 squares-search of the PD stage 1 grid yielded one crystalline COD ghost, 3 crystalline TiO_2 particles and 3

crystalline iron oxide particles; the 3 squares-search of the PD stage 2 grid yielded one crystalline COD ghost, 4 crystalline TiO_2 particles and 2 crystalline iron oxide particles; the single-square search of the PD stage 4 grid yielded one crystalline TiO_2 particle and 2 crystalline iron oxide particles; and the search of only a part of a single square of the PD stage 5 grid yielded 3 COD ghosts, 4 TiO_2 and 2 iron oxide, for a total of 5 COD, 12 TiO_2 and 9 Fe(O)OH particles. Of the 4 x 314 = 1,256 squares of the 4 grids 7 were fully searched and one was partially searched, meaning that the fraction of the searched squares was about 7.5/1,256=0.006. With about 0.01 of the volume of the dispersions having been applied to 4 grids, the fraction of the observed crystals was 6 x 10^{-5}, meaning that each observed crystal represented about 1.6 x 10^4 crystals in the 4 x 5 mg = 20 mg total tissue sampled, or 8 x 10^5 crystalline particles per gram of *substantia nigra*. Because we find > 5 COD, > 12 TiO_2 and > 9 iron oxide particles, there are more than 4 x 10^6 COD, 10^7 TiO_2 and 7 x 10^6 iron oxide particles per gram of *substantia nigra*.

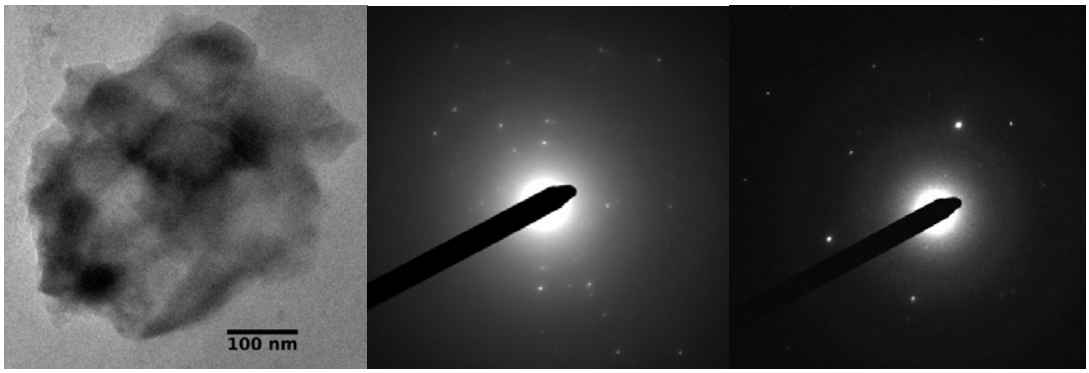

Figure 2. *Left.* Ghost of a COD particle of the PD stage 5 *substantia nigra* containing 53 ± 5 weight % calcium (excl. carbon), increasing as the particle decomposes under the electron-beam to 64 ± 5 weight %. *Center and right:* Changing electron diffraction patterns of the unstable particle when heated by e-beam under the TEM chamber's 10^{-8} torr vacuum.

Figure 1 shows a TEM image of the crystals in the PD stage 5 specimen with calcium-, titanium-, and iron-rich crystalline particles in the same field. The calcium-containing crystalline particles, an example of which is seen in Figure 2, did not contain phosphorus above the background-level, ruling out their being calcium phosphate, apatite or calcium pyrophosphate crystals. In the 10^{-8} torr vacuum of the chamber of the transmission electron microscope the imaged COD crystals promptly pulverized as they are dehydrated, then gradually lost CO_2 and CO approaching, when completely de-gassed, the expected 71 weight % of CaO, their electron diffraction patterns changing while they are de-gassed. (Figure 2)

Figure 3 shows crystalline TiO_2 particles of PD stages 1,2, 4 and 5 *substantia nigra*. Their 42 weight % -54 weight % titanium content is less than the expected 59.5 weight % for TiO_2, implying that they are protein-coated. The difference between the observed 46.5 average weight % TiO_2 and the expected 59.5 % is consistent with protein constituting about 20 % of the mass of the particles. As seen in Figure 3, the adsorbed protein is thick enough to round the all edges and corners of all the face-sharing mono-

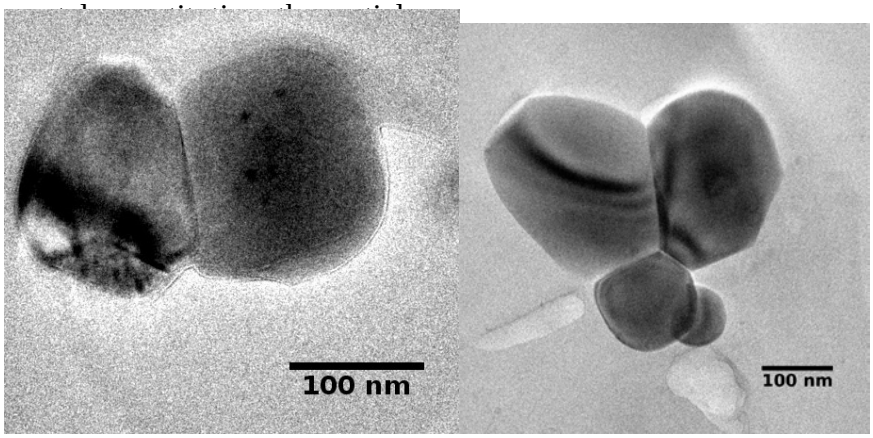

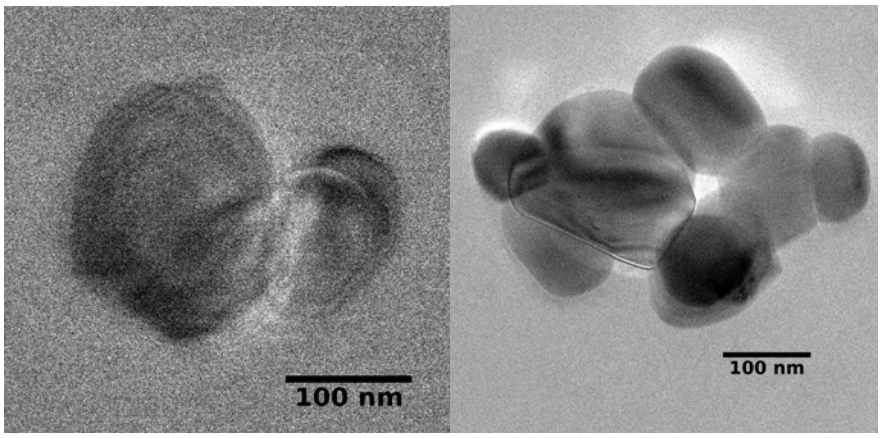

Figure 3. Crystalline TiO_2 particles of the PD *substantia nigra*. *Top left*, from the PD stage 1 specimen, containing 54 ± 5 weight % titanium; *Top right*, from the PD stage 2 specimen, containing 42 ± 5 weight % titanium; *Bottom left*, from the PD stage 4 specimen, containing 46 ± 5 weight % titanium; Bottom right, from the PD stage 5 specimen, containing 44 ± 5 weight % titanium. The expected weight % of titanium in TiO_2 is 59.5 %, implying that all particles are protein-coated. Protein-coating is also evident from the smoothing of the edges and corners of the crystals.

Figure 4 shows crystalline iron oxide particles of the PD stages 1,2 and 4 *substantia nigra* grids. Compositions of two are consistent with the 63 weight % iron content of Fe(O)OH, the mineral Goethite; the third shows only 51 ± 5 weight % iron content, attributed to the particle being protein-coated. Biogenic iron oxide crystals are known to abound in the human brain. [63, 64] The average iron content of 57.6 ± 5 % suggests, but does not establish, that the crystals are coated with protein constituting less than 10 % of the particle-mass.

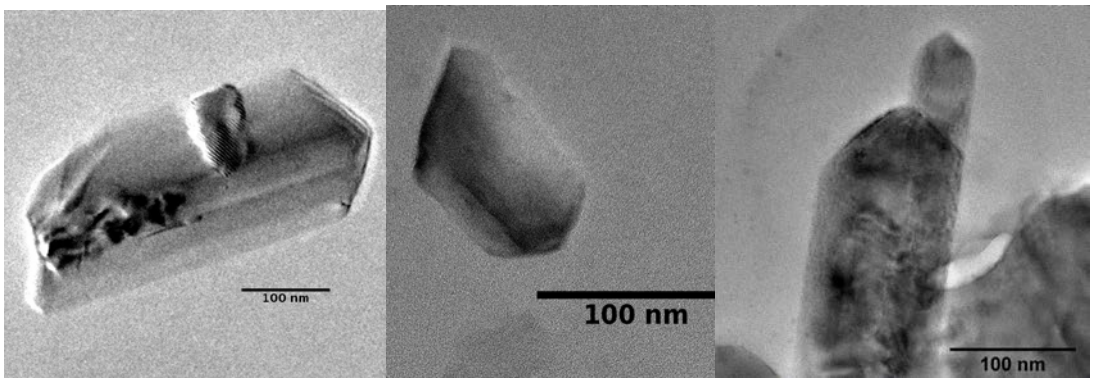

Figure 4. Crystalline iron oxide particles of the PD *substantia nigra*. *Left*, from the PD stage 1 specimen, containing 61 ± 5 weight % iron consistent with the expected 63.6 weight % in Goethite, Fe(O)OH. *Center*, from the PD stage 2 specimen, containing 51 ± 5 weight % Fe. The less than theoretical weight % of iron implies that the crystal is protein-coated. *Right*, from the PD stage 4 specimen, Fe-content 61 ±5 weight %, consistent with the expected for Goethite, Fe(O)OH. The crystals exhibit both sharp and rounded corners and edges implying that only some adsorb a thick protein layer.

Discussion

The results show that the human PD *substantia nigra* contains submicron-sized crystalline COD and TiO_2 particles. Both are phagocytized, [25, 35-39] the TiO_2 also by microglia [20, 40]. In mice, activation of microglial NLRP3 inflammasome by misfolded α-synuclein causes the death of proximal dopaminergic neurons. [1, 3, 8-11] The found TiO_2 particles are coated with a protein-layer, constituting about 20 % of their mass. TiO_2, shown to adsorb and orient peptides and polymers [27-29] could also adsorb α-synuclein or its precursor peptides. It remains to be seen if the protein-layer found on the TiO_2 crystals is or comprises α-synuclein and if it does, whether the α-synuclein coating is misfolded.

In humans COD inflammasome-activation causes nephropathy. [24] Just as the phagocytized α-synuclein activates the microglial NLRP3 inflammasome. Both COD and TiO_2 are phagocytized and NLRP3 inflammasome activating. [20, 24, 25, 38, 41-47] If they activate also the microglial NLRP3 inflammasome, as is likely, proximal dopaminergic neurons would die. Because the number of microglia approaches the number of neuronal cells of the brain [65] each dopaminergic cell has on the average more than one proximal microglial cell. Consequently, in absence of segregation of the dopaminergic substantia nigra cells and the glia, death of the majority of the dopaminergic cells is expected when the NLRP3 inflammasome is activated in a large fraction of the glia. The human brain weighs about 1.5 kg and the count of its microglia is about 5×10^{10}[65], meaning that there about 3×10^7 microglia per gram. Considering that we find > 4×10^6 COD and > 9.6×10^6 TiO_2 particles per gram of *substantia nigra*, the number-density of particles suffices for the killing of a large fraction the dopaminergic cells.

Hydrated calcium oxalate precipitates when the solubility product of the concentrations of Ca^{2+} and oxalate is exceeded, that is when the Ca^{2+} concentration is very high, or the oxalate concentration is high, or when both concentrations are moderately elevated. COD can precipitate if Ca^{2+} stored in the endoplasmic reticulum is released into its cytoplasm, or if oxalate is excessively formed from ascorbate or citrate. Of the two, ascorbate is the more likely precursor, because in stimulated murine macrophages its concentration is about 100-fold higher than it is in the extracellular fluid, reaching 10 mM. [66] It is, therefore not surprising that a massive ascorbic acid overdose caused lethal calcium oxalate nephropathy in a patient.[67] In the ascorbate pathway, part of the ascorbate is oxidized to dehydroascorbate and is converted to 2,3-diketogluconate. 2,3-diketogluconate is oxidized by H_2O_2 to oxalate. [68] Oxalate production is pronounced in inflammatory M1 macrophages, but not in non-inflammatory M2 macrophages [69]; such may be the case also in stimulated microglia. Because COD stimulates

macrophages. [37] An amplified inflammatory feedback loop results when more 2,3-diketogluconate-oxidizing H_2O_2 is produced by repeated O_2-oxidation of the ascorbate-reduced pre-melanin, the pre-melamine being produced by O_2-oxidation of dopamine. [70] The loop is further amplified by activation of the glia by the formed COD.

Titanium compounds have no known role in human physiology, although implanted titanium alloys do produce erosion products found in the marrow[71] and result in measurable plasma-concentrations of titanium compounds.[72] Reviews of the toxicology of titanium focus, however, on ingested and inhaled white TiO_2 pigment particles, [61, 73-75] widely used as white pigments in foods and medications. The ingested pigment particles pass into the bloodstream[76] and are transported to the human liver, [77] spleen[77] and pancreas[78]. In animals inhaling the pigment, TiO_2 particles were detected also in the brain.[61] Although the TiO_2 particles are phagocytized and activate the NLRP3 inflammasome [20, 41, 47, 79, 80] their human pathogenicity is less well established than that of the COD particles.[37, 69, 81] Nevertheless, treatment of dopaminergic neurons with TiO_2 has been shown to increase α-synuclein expression and to cause its aggregation in a dose-dependent manner. [26] Future studies might show if the observed thick protein-coating of the TiO_2 particles (Figure 3) is the misfolded α-synuclein of Lewy-bodies. If this would be so, TiO_2 might template the PD-underlying misfolding of this PD-hallmark protein.

Biogenic submicron iron oxide particles are well known residents of the human brain [63, 82] In the rat, brain nasally-instilled iron oxide damages dopaminergic neurons. [83] There are, however, no reports establishing that iron oxide activates the NLRP3 inflammasome. Siderosis, resulting of inhalation of iron oxide crystals by miners and steelworkers, is a relatively mild and reversible disease.

In conclusion, should future studies establish that the crystalline COD particles that were found in the *substantia nigra* cause PD, mitigation by long-known and inexpensive means of reducing COD-caused urolithiasis, such avoidance of hypomagnesemia, [84-87] could be considered. Should future studies establish that TiO_2 particles cause PD, alternative white foods and medication colorants should be considered.

Acknowledgement.

The authors thank Dr. Karalee Jarvis for her expert guidance of the transmission electron microscopy.

Financial support statement.

AH thanks the Welch Foundation (Grant F-1131) for supporting this study.

Conflict of Interest Statement.

AH is employed by the University of Texas at Austin, by Synagile Corp. and consults to Abbott Diabetes Care. The authors declare no conflict of interest.

References.

1. Codolo G, Plotegher N, Pozzobon T, Brucale M, Tessari I, Bubacco L, et al. Triggering of inflammasome by aggregated α-synuclein, an inflammatory response in synucleinopathies. PloS one. 2013;8:e55375. doi: 10.1371/journal.pone.0055375.
2. Heneka MT, Kummer MP, Latz E, Gustin A, Kirchmeyer M, Koncina E, et al. Innate immune activation in neurodegenerative disease. NLRP3 Inflammasome Is Expressed and Functional in Mouse Brain Microglia but Not in Astrocytes. Nat Rev Immunol. 2014;14(7):463-77. Epub 2014/06/26. doi: 10.1038/nri3705. PubMed PMID: 24962261.
3. Wang L, Zhai YQ, Xu LL, Qiao C, Sun XL, Ding JH, et al. Metabolic inflammation exacerbates dopaminergic neuronal degeneration in response to acute MPTP challenge in type 2 diabetes mice. Exp Neurol. 2014;251:22-9. Epub 2013/11/14. doi: 10.1016/j.expneurol.2013.11.001. PubMed PMID: 24220636.

4. Gustot A, Gallea JI, Sarroukh R, Celej MS, Ruysschaert JM, Raussens V. Amyloid fibrils are the molecular trigger of inflammation in Parkinson's disease. The Biochemical journal. 2015;471(3):323-33. Epub 2015/08/15. doi: 10.1042/bj20150617. PubMed PMID: 26272943.
5. Wang W, Nguyen LT, Burlak C, Chegini F, Guo F, Chataway T, et al. Caspase-1 causes truncation and aggregation of the Parkinson's disease-associated protein alpha-synuclein. Proceedings of the National Academy of Sciences of the United States of America. 2016;113(34):9587-92. Epub 2016/08/03. doi: 10.1073/pnas.1610099113. PubMed PMID: 27482083; PubMed Central PMCID: PMC5003239.
6. Shao QH, Zhang XL, Yang PF, Yuan YH, Chen NH. Amyloidogenic proteins associated with neurodegenerative diseases activate the NLRP3 inflammasome. International immunopharmacology. 2017;49:155-60. Epub 2017/06/09. doi: 10.1016/j.intimp.2017.05.027. PubMed PMID: 28595078.
7. Martinez EM, Young AL, Patankar YR, Berwin BL, Wang L, von Herrmann KM, et al. Nlrp3 is required for inflammatory changes and nigral cell loss resulting from chronic intragastric rotenone exposure in mice. Toxicol Sci. 2017;159(1):64-75. doi: 10.1093/toxsci/kfx117.
8. Mo Y, Xu E, Wei R, Le B, Song L, Li D, et al. Bushen-Yizhi Formula Alleviates Neuroinflammation via Inhibiting NLRP3 Inflammasome Activation in a Mouse Model of Parkinson's Disease. Evidence-based complementary and alternative medicine : eCAM. 2018;2018:3571604. Epub 2018/09/19. doi: 10.1155/2018/3571604. PubMed PMID: 30224927; PubMed Central PMCID: PMCPMC6129340.
9. Qiao C, Zhang Q, Jiang Q, Zhang T, Chen M, Fan Y, et al. Inhibition of the hepatic Nlrp3 protects dopaminergic neurons via attenuating systemic inflammation in a MPTP/p mouse model of Parkinson's disease. Journal of neuroinflammation. 2018;15(1):193. Epub 2018/07/04. doi: 10.1186/s12974-018-1236-z. PubMed PMID: 29966531; PubMed Central PMCID: PMCPMC6029067.
10. Lee E, Hwang I, Park S, Hong S, Hwang B, Cho Y, et al. MPTP-driven NLRP3 inflammasome activation in microglia plays a central role in dopaminergic neurodegeneration. Cell death and differentiation. 2018. Epub 2018/05/23. doi: 10.1038/s41418-018-0124-5. PubMed PMID: 29786072.
11. Gordon R, Albornoz EA, Christie DC, Kumar V, Woodruff TM, Gordon R, et al. Inflammasome inhibition prevents α-synuclein pathology and dopaminergic neurodegeneration in mice. Sci Transl Med. 2018;10(465).
12. Heneka MT, McManus RM, Latz E. Inflammasome signalling in brain function and neurodegenerative disease. Nat Rev Neurosci. 2018;19(10):610-21. doi: 10.1038/s41583-018-0055-7.
13. Prusiner SB. A Unifying Role for Prions in Neurodegenerative Diseases. Science. 2012;336(6088):1511. doi: 10.1126/science.1222951.
14. Olanow CW, Brundin P. Parkinson's disease and alpha synuclein: is Parkinson's disease a prion-like disorder? Movement disorders : official journal of the Movement Disorder Society. 2013;28(1):31-40. Epub 2013/02/08. doi: 10.1002/mds.25373. PubMed PMID: 23390095.
15. Steiner JA, Quansah E, Brundin P. The concept of alpha-synuclein as a prion-like protein: ten years after. Cell and tissue research. 2018;373(1):161-73. Epub 2018/02/27. doi: 10.1007/s00441-018-2814-1. PubMed PMID: 29480459.
16. Martinon F, Petrilli V, Mayor A, Tardivel A, Tschopp J. Gout-associated uric acid crystals activate the NALP3 inflammasome. Nature. 2006;440(7081):237-41. Epub 2006/01/13. doi: 10.1038/nature04516. PubMed PMID: 16407889.
17. Hornung V, Bauernfeind F, Halle A, Samstad EO, Kono H, Rock KL, et al. Silica crystals and aluminum salts activate the NALP3 inflammasome through phagosomal destabilization. Nature immunology. 2008;9(8):847-56. Epub 2008/07/08. doi: 10.1038/ni.1631. PubMed PMID: 18604214; PubMed Central PMCID: PMCPMC2834784.
18. Ea HK, Liote F, Savage CD, Lopez-Castejon G, Denes A, Brough D. Advances in understanding calcium-containing crystal disease. NLRP3-Inflammasome Activating DAMPs Stimulate an Inflammatory Response

in Glia in the Absence of Priming Which Contributes to Brain Inflammation after Injury. Curr Opin Rheumatol. 2009;21(2):150-7. Epub 2009/04/03. doi: 10.1097/BOR.0b013e3283257ba9. PubMed PMID: 19339926.
19. Rajamaki K, Lappalainen J, Oorni K, Valimaki E, Matikainen S, Kovanen PT, et al. Cholesterol crystals activate the NLRP3 inflammasome in human macrophages: a novel link between cholesterol metabolism and inflammation. PloS one. 2010;5(7):e11765. Epub 2010/07/30. doi: 10.1371/journal.pone.0011765. PubMed PMID: 20668705; PubMed Central PMCID: PMCPMC2909263.
20. Winter M, Beer HD, Hornung V, Kramer U, Schins RP, Forster I. Activation of the inflammasome by amorphous silica and TiO2 nanoparticles in murine dendritic cells. Nanotoxicology. 2011;5(3):326-40. Epub 2010/09/18. doi: 10.3109/17435390.2010.506957. PubMed PMID: 20846021.
21. Narayan S, Pazar B, Ea HK, Kolly L, Bagnoud N, Chobaz V, et al. Octacalcium phosphate crystals induce inflammation in vivo through interleukin-1 but independent of the NLRP3 inflammasome in mice. Arthritis and rheumatism. 2011;63(2):422-33. Epub 2011/02/01. doi: 10.1002/art.30147. PubMed PMID: 21279999.
22. Pazar B, Ea HK, Narayan S, Kolly L, Bagnoud N, Chobaz V, et al. Basic calcium phosphate crystals induce monocyte/macrophage IL-1beta secretion through the NLRP3 inflammasome in vitro. Journal of immunology (Baltimore, Md : 1950). 2011;186(4):2495-502. Epub 2011/01/18. doi: 10.4049/jimmunol.1001284. PubMed PMID: 21239716.
23. Prencipe G, Caiello I, Cherqui S, Whisenant T, Petrini S, Emma F, et al. Inflammasome activation by cystine crystals: implications for the pathogenesis of cystinosis. Journal of the American Society of Nephrology : JASN. 2014;25(6):1163-9. Epub 2014/02/15. doi: 10.1681/asn.2013060653. PubMed PMID: 24525029; PubMed Central PMCID: PMCPMC4033370.
24. Joshi S, Wang W, Peck AB, Khan SR. Activation of the NLRP3 Inflammasome in Association with Calcium Oxalate Crystal Induced Reactive Oxygen Species in Kidneys. J Urol (N Y, NY, U S). 2015;193:1684-91. doi: 10.1016/j.juro.2014.11.093.
25. Anders HJ, Suarez-Alvarez B, Grigorescu M, Foresto-Neto O, Steiger S, Desai J, et al. The macrophage phenotype and inflammasome component NLRP3 contributes to nephrocalcinosis-related chronic kidney disease independent from IL-1-mediated tissue injury. Calcium Oxalate Stone Fragment and Crystal Phagocytosis by Human Macrophages. Kidney Int. 2018;93(3):656-69. Epub 2018/03/15. doi: 10.3389/fimmu.2018.00316. PubMed PMID: 29241624; PubMed Central PMCID: PMC5835051.
26. Wu J, Xie H. Effects of titanium dioxide nanoparticles on alpha-synuclein aggregation and the ubiquitin-proteasome system in dopaminergic neurons. Artificial cells, nanomedicine, and biotechnology. 2016;44(2):690-4. Epub 2014/11/12. doi: 10.3109/21691401.2014.980507. PubMed PMID: 25386730.
27. Forstater JH, Kleinhammes A, Wu Y. Self-assembly of protein-based biomaterials initiated by titania nanotubes. Langmuir : the ACS journal of surfaces and colloids. 2013;29(48):15013-21. Epub 2013/11/10. doi: 10.1021/la403414t. PubMed PMID: 24200123.
28. Mirau PA, Naik RR, Gehring P. Structure of peptides on metal oxide surfaces probed by NMR. Journal of the American Chemical Society. 2011;133(45):18243-8. Epub 2011/10/11. doi: 10.1021/ja205454t. PubMed PMID: 21981074.
29. Raghava S, Singh PK, Ranga Rao A, Dutta V, Gupta MN. Nanoparticles of unmodified titanium dioxide facilitate protein refolding. J Mater Chem. 2009;19(Copyright (C) 2017 American Chemical Society (ACS). All Rights Reserved.):2830-4. doi: 10.1039/b817306k.
30. Sun XY, Gan QZ, Ouyang JM. Calcium oxalate toxicity in renal epithelial cells: the mediation of crystal size on cell death mode. Cell Death Discov. 2015;1:15055. Epub 2015/01/01. doi: 10.1038/cddiscovery.2015.55. PubMed PMID: 27551481; PubMed Central PMCID: PMC4979418.
31. Hoffman GS, Schumacher HR, Paul H, Cherian V, Reed R, Ramsay AG, et al. Calcium oxalate microcrystalline-associated arthritis in end-stage renal disease. Annals of internal medicine. 1982;97(1):36-42. Epub 1982/07/01. PubMed PMID: 7092004.

32. Verkoelen CF, Romijn JC. Oxalate transport and calcium oxalate renal stone disease. Urological research. 1996;24(4):183-91. Epub 1996/01/01. PubMed PMID: 8873376.
33. Small KW, Letson R, Scheinman J. Ocular findings in primary hyperoxaluria. Archives of ophthalmology (Chicago, Ill : 1960). 1990;108(1):89-93. Epub 1990/01/01. PubMed PMID: 2297338.
34. Farreli J, Shoemaker JD, Otti T, Jordan W, Schoch L, Neu LT, et al. Primary hyperoxaluria in an adult with renal failure, livedo reticularis, retinopathy, and peripheral neuropathy. American journal of kidney diseases : the official journal of the National Kidney Foundation. 1997;29(6):947-52. Epub 1997/06/01. PubMed PMID: 9186083.
35. Long TC, Saleh N, Tilton RD, Lowry GV, Veronesi B, Bechmann I, et al. Titanium dioxide (P25) produces reactive oxygen species in immortalized brain microglia (BV2): implications for nanoparticle neurotoxicity. Astrocytes and microglial cells incorporate degenerating fibers following entorhinal lesion: a light, confocal, and electron microscopical study using a phagocytosis-dependent labeling technique. Environ Sci Technol. 2006;40(14):4346-52. Epub 2007/11/17. doi: 10.1289/ehp.10216. PubMed PMID: 16903269; PubMed Central PMCID: PMC2072833.
36. Morishige T, Yoshioka Y, Tanabe A, Yao X, Tsunoda S, Tsutsumi Y, et al. Titanium dioxide induces different levels of IL-1beta production dependent on its particle characteristics through caspase-1 activation mediated by reactive oxygen species and cathepsin B. Biochem Biophys Res Commun. 2010;392(2):160-5. Epub 2010/01/12. doi: 10.1016/j.bbrc.2009.12.178. PubMed PMID: 20059972.
37. Kusmartsev S, Dominguez-Gutierrez PR, Canales BK, Bird VG, Vieweg J, Khan SR. Calcium Oxalate Stone Fragment and Crystal Phagocytosis by Human Macrophages. The Journal of urology. 2016;195(4 Pt 1):1143-51. Epub 2015/12/03. doi: 10.1016/j.juro.2015.11.048. PubMed PMID: 26626217; PubMed Central PMCID: PMC4882284.
38. Honarpisheh M, Foresto-Neto O, Desai J, Steiger S, Gomez LA, Popper B, et al. Phagocytosis of environmental or metabolic crystalline particles induces cytotoxicity by triggering necroptosis across a broad range of particle size and shape. Sci Rep. 2017;7(1):15523. Epub 2018/10/26. doi: 10.3389/fimmu.2018.02248. PubMed PMID: 29138474; PubMed Central PMCID: PMC6189479.
39. Dominguez-Gutierrez PR, Kusmartsev S, Canales BK, Khan SR. Calcium Oxalate Differentiates Human Monocytes Into Inflammatory M1 Macrophages. Front Immunol. 2018;9:1863. PubMed PMID: 30186283.
40. Zeman T, Loh EW, Cierny D, Sery O, Deora V, Albornoz EA, et al. Penetration, distribution and brain toxicity of titanium nanoparticles in rodents' body: a review. IET Nanobiotechnol. 2018;12(6):695-700. Epub 2018/08/15. doi: 10.1049/iet-nbt.2017.0109. PubMed PMID: 30104440.
41. Yazdi AS, Guarda G, Riteau N, Drexler SK, Tardivel A, Couillin I, et al. Nanoparticles activate the NLR pyrin domain containing 3 (Nlrp3) inflammasome and cause pulmonary inflammation through release of IL-1alpha and IL-1beta. Proceedings of the National Academy of Sciences of the United States of America. 2010;107(45):19449-54. Epub 2010/10/27. doi: 10.1073/pnas.1008155107. PubMed PMID: 20974980; PubMed Central PMCID: PMCPMC2984140.
42. Mulay SR, Kulkarni OP, Rupanagudi KV, Migliorini A, Darisipudi MN, Vilaysane A, et al. Calcium oxalate crystals induce renal inflammation by NLRP3-mediated IL-1β secretion. J Clin Invest. 2013;123:236-46. doi: 10.1172/jci63679.
43. Knauf F, Asplin JR, Granja I, Schmidt IM, Moeckel GW, David RJ, et al. NALP3-mediated inflammation is a principal cause of progressive renal failure in oxalate nephropathy. Kidney Int. 2013;84:895-901.
44. Mulay SR, Desai J, Kumar SV, Eberhard JN, Thomasova D, Romoli S, et al. Cytotoxicity of crystals involves RIPK3-MLKL-mediated necroptosis. Nat Commun. 2016;7:10274. doi: 10.1038/ncomms10274.
45. Ermer T, Eckardt K-U, Aronson PS, Knauf F. Oxalate, inflammasome, and progression of kidney disease. Curr Opin Nephrol Hypertens. 2016;25:363-71. doi: 10.1097/mnh.0000000000000229.

46. Ruiz PA, Moron B, Becker HM, Lang S, Atrott K, Spalinger MR, et al. Titanium dioxide nanoparticles exacerbate DSS-induced colitis: role of the NLRP3 inflammasome. . Gut. 2017;66(7):1216-24. Epub 2016/02/06. doi: 10.1136/gutjnl-2015-310297. PubMed PMID: 26848183.
47. Kim BG, Lee PH, Lee SH, Park MK, Jang AS. Effect of TiO(2) Nanoparticles on Inflammasome-Mediated Airway Inflammation and Responsiveness. Allergy Asthma Immunol Res. 2017;9(3):257-64. Epub 2017/03/16. doi: 10.4168/aair.2017.9.3.257. PubMed PMID: 28293932; PubMed Central PMCID: PMCPMC5352577.
48. Gonzalez JE, Caldwell RG, Valaitis J. Calcium oxalate crystals in the breast. Pathology and significance. The American journal of surgical pathology. 1991;15(6):586-91. Epub 1991/06/01. PubMed PMID: 2031531.
49. Froberg K, Dorion RP, McMartin KE. The role of calcium oxalate crystal deposition in cerebral vessels during ethylene glycol poisoning. Clinical toxicology (Philadelphia, Pa). 2006;44(3):315-8. Epub 2006/06/06. PubMed PMID: 16749551.
50. Linnes MP, Krambeck AE, Cornell L, Williams JC, Jr., Korinek M, Bergstralh EJ, et al. Phenotypic characterization of kidney stone formers by endoscopic and histological quantification of intrarenal calcification. Kidney Int. 2013;84(4):818-25. Epub 2013/05/24. doi: 10.1038/ki.2013.189. PubMed PMID: 23698231; PubMed Central PMCID: PMCPMC3784621.
51. Haqqani MT. Crystals in brain and meninges in primary hyperoxaluria and oxalosis. Journal of clinical pathology. 1977;30(1):16-8. PubMed PMID: 838867.
52. Armstrong EJ, Engelhart DA, Jenkins AJ, Balraj EK. Homicidal ethylene glycol intoxication: a report of a case. The American journal of forensic medicine and pathology. 2006;27(2):151-5. Epub 2006/06/02. doi: 10.1097/01.paf.0000203221.17854.38. PubMed PMID: 16738434.
53. Gaultier M, Conso F, Rudler M, Leclerc JP, Mellerio F. [Acute ethylene glycol poisoning]. European journal of toxicology and environmental hygiene Journal europeen de toxicologie. 1976;9(6):373-9. Epub 1976/11/01. PubMed PMID: 1026432.
54. Peiffer J, Danner E, Schmidt PF. Oxalate-induced encephalitic reactions to polyol-containing infusions during intensive care. Clinical neuropathology. 1984;3(2):76-87. Epub 1984/03/01. PubMed PMID: 6424993.
55. Zarembski PM, Hodgkinson A. Plasma oxalic acid and calcium levels in oxalate poisoning. Journal of clinical pathology. 1967;20(3):283-5. Epub 1967/05/01. PubMed PMID: 5602563; PubMed Central PMCID: PMCPMC473488.
56. Leth PM, Gregersen M. Ethylene glycol poisoning. Forensic science international. 2005;155(2-3):179-84. Epub 2005/10/18. doi: 10.1016/j.forsciint.2004.11.012. PubMed PMID: 16226155.
57. Introna F, Jr., Smialek JE. Antifreeze (ethylene glycol) intoxications in Baltimore. Report of six cases. Acta morphologica Hungarica. 1989;37(3-4):245-63. Epub 1989/01/01. PubMed PMID: 2486465.
58. Reddy NJ, Lewis LD, Gardner TB, Osterling W, Eskey CJ, Nierenberg DW. Two cases of rapid onset Parkinson's syndrome following toxic ingestion of ethylene glycol and methanol. Clin Pharmacol Ther (N Y, NY, U S). 2007;81(Copyright (C) 2017 American Chemical Society (ACS). All Rights Reserved.):114-21. doi: 10.1038/sj.clpt.6100013.
59. Wang J, Chen C, Liu Y, Jiao F, Li W, Lao F, et al. Potential neurological lesion after nasal instillation of TiO_2 nanoparticles in the anatase and rutile crystal phases. Toxicol Lett. 2008;183(1-3):72-80. doi: 10.1016/j.toxlet.2008.10.001. PubMed PMID: 18992307.
60. Schmid O, Moller W, Semmler-Behnke M, Ferron GA, Karg E, Lipka J, et al. Dosimetry and toxicology of inhaled ultrafine particles. Biomarkers. 2009;14 Suppl 1(14):67-73. Epub 2009/11/26. doi: 10.1080/13547500902965617. PubMed PMID: 19604063; PubMed Central PMCID: PMC3804071.

61. Czajka M, Sawicki K, Sikorska K, Popek S, Kruszewski M, Kapka-Skrzypczak L. Toxicity of titanium dioxide nanoparticles in central nervous system. Toxicol In Vitro. 2015;29(5):1042-52. Epub 2015/04/23. doi: 10.1016/j.tiv.2015.04.004. PubMed PMID: 25900359.
62. Hu Q, Guo F, Zhao F, Fu Z. Effects of titanium dioxide nanoparticles exposure on parkinsonism in zebrafish larvae and PC12. Chemosphere. 2017;173:373-9.
63. Kirschvink JL, Kobayashi-Kirschvink A, Woodford BJ. Magnetite biomineralization in the human brain. Proceedings of the National Academy of Sciences of the United States of America. 1992;89(16):7683-7. PubMed PMID: 1502184.
64. Dobson J. Nanoscale biogenic iron oxides and neurodegenerative disease. FEBS Lett. 2001;496:1-5. doi: 10.1016/s0014-5793(01)02386-9.
65. von Bartheld CS, Bahney J, Herculano-Houzel S. The search for true numbers of neurons and glial cells in the human brain: A review of 150 years of cell counting. The Journal of comparative neurology. 2016;524(18):3865-95. Epub 2016/05/18. doi: 10.1002/cne.24040. PubMed PMID: 27187682; PubMed Central PMCID: PMCPMC5063692.
66. May JM, Huang J, Qu ZC. Macrophage uptake and recycling of ascorbic acid: response to activation by lipopolysaccharide. Free Radic Biol Med. 2005;39(11):1449-59. Epub 2005/11/09. doi: 10.1016/j.freeradbiomed.2005.07.006. PubMed PMID: 16274880.
67. Wong K, Thomson C, Bailey RR, McDiarmid S, Gardner J, Lawton JM, et al. Acute oxalate nephropathy after a massive intravenous dose of vitamin C. Aust N Z J Med. 1994;24(4):410-1. Epub 1994/08/01. PubMed PMID: 7980244.
68. Knight J, Madduma-Liyanage K, Mobley JA, Assimos DG, Holmes RP. Ascorbic acid intake and oxalate synthesis. Urolithiasis. 2016;44(4):289-97. Epub 2016/03/22. doi: 10.1007/s00240-016-0868-7. PubMed PMID: 27002809.
69. Taguchi K, Okada A, Hamamoto S, Unno R, Moritoki Y, Ando R, et al. M1/M2-macrophage phenotypes regulate renal calcium oxalate crystal development. Sci Rep. 2016;6:35167. Epub 2016/10/13. doi: 10.1038/srep35167. PubMed PMID: 27731368; PubMed Central PMCID: PMCPMC5059697.
70. Pileblad E, Slivka A, Bratvold D, Cohen G. Studies on the autoxidation of dopamine: interaction with ascorbate. Archives of biochemistry and biophysics. 1988;263(2):447-52. Epub 1988/06/01. PubMed PMID: 3377513.
71. Hall DJ, Pourzal R, Jacobs JJ, Urban RM. Metal wear particles in hematopoietic marrow of the axial skeleton in patients with prior revision for mechanical failure of a hip or knee arthroplasty. Journal of Biomedical Materials Research Part B: Applied Biomaterials. 2018;0(0). doi: 10.1002/jbm.b.34285.
72. Curtin JP, Wang M, Cheng T, Jin L, Sun H. The role of citrate, lactate and transferrin in determining titanium release from surgical devices into human serum. JBIC Journal of Biological Inorganic Chemistry. 2018;23(3):471-80. doi: 10.1007/s00775-018-1557-5.
73. Jovanovic B. Critical review of public health regulations of titanium dioxide, a human food additive. Integr Environ Assess Manag. 2015;11(1):10-20. Epub 2014/08/06. doi: 10.1002/ieam.1571. PubMed PMID: 25091211; PubMed Central PMCID: PMCPMC4309481.
74. Grande F, Tucci P. Titanium Dioxide Nanoparticles: a Risk for Human Health? Mini Rev Med Chem. 2016;16(9):762-9. Epub 2016/03/22. PubMed PMID: 26996620.
75. Winkler HC, Notter T, Meyer U, Naegeli H. Critical review of the safety assessment of titanium dioxide additives in food. J Nanobiotechnology. 2018;16(1):51. Epub 2018/06/03. doi: 10.1186/s12951-018-0376-8. PubMed PMID: 29859103; PubMed Central PMCID: PMCPMC5984422.
76. Pele LC, Thoree V, Bruggraber SF, Koller D, Thompson RP, Lomer MC, et al. Pharmaceutical/food grade titanium dioxide particles are absorbed into the bloodstream of human volunteers. Part Fibre Toxicol.

2015;12:26. Epub 2015/09/04. doi: 10.1186/s12989-015-0101-9. PubMed PMID: 26330118; PubMed Central PMCID: PMCPMC4557898.
77. Heringa MB, Peters RJB, Bleys R, van der Lee MK, Tromp PC, van Kesteren PCE, et al. Detection of titanium particles in human liver and spleen and possible health implications. Part Fibre Toxicol. 2018;15(1):15. Epub 2018/04/13. doi: 10.1186/s12989-018-0251-7. PubMed PMID: 29642936; PubMed Central PMCID: PMCPMC5896156.
78. Heller A, Jarvis K, Coffman SS. Association of Type 2 Diabetes with Submicron Titanium Dioxide Crystals in the Pancreas. Chem Res Toxicol. 2018;31(6):506-9. Epub 2018/05/25. doi: 10.1021/acs.chemrestox.8b00047. PubMed PMID: 29792697.
79. Hamilton RF, Wu N, Porter D, Buford M, Wolfarth M, Holian A. Particle length-dependent titanium dioxide nanomaterials toxicity and bioactivity. Part Fibre Toxicol. 2009;6:35.
80. Tsugita M, Morimoto N, Nakayama M. SiO2 and TiO2 nanoparticles synergistically trigger macrophage inflammatory responses. Part Fibre Toxicol. 2017;14(1):11. Epub 2017/04/13. doi: 10.1186/s12989-017-0192-6. PubMed PMID: 28399878; PubMed Central PMCID: PMC5387387.
81. Maguire R. On Oxaluria and the Treatment of Calcium Oxalate Deposit from the Urine, with a Method for the Solution of Calcium Oxalate Calculus whilst in the Urinary Passages. Proc R Soc Med. 1910;3(Med Sect):1-24. PubMed PMID: 19974465.
82. Schultheiss-Grassi PP, Wessiken R, Dobson J. TEM investigations of biogenic magnetite extracted from the human hippocampus. Biochim Biophys Acta, Gen Subj. 1999;1426:212-6. doi: 10.1016/s0304-4165(98)00160-3.
83. Wu J, Ding T, Sun J. Neurotoxic potential of iron oxide nanoparticles in the rat brain striatum and hippocampus. NeuroToxicology. 2013;34:243-53. doi: 10.1016/j.neuro.2012.09.006.
84. Berg W, Hesse A, Schneider HJ. A contribution to the formation mechanism of calcium oxalate urinary calculi. III. On the role of magnesium in the formation of oxalate calculi. Urological research. 1976;4(4):161-7. Epub 1976/01/01. PubMed PMID: 14432.
85. Drach GW. Contribution to therapeutic decisions of ratios, absolute values and other measures of calcium, magnesium, urate or oxalate balance in stone formers. The Journal of urology. 1976;116(3):338-40. Epub 1976/09/01. PubMed PMID: 957503.
86. Berg W, Bothor C, Pirlich W, Janitzky V. Influence of magnesium on the absorption and excretion of calcium and oxalate ions. European urology. 1986;12(4):274-82. Epub 1986/01/01. PubMed PMID: 3743598.
87. Ettinger B, Pak CY, Citron JT, Thomas C, Adams-Huet B, Vangessel A. Potassium-magnesium citrate is an effective prophylaxis against recurrent calcium oxalate nephrolithiasis. The Journal of urology. 1997;158(6):2069-73. Epub 1997/11/20. PubMed PMID: 9366314.